P12R.7   POWER CALIBRATION OF VHF STRATOSPHERIC-TROPOSPHERIC RADARS

Edwin F. Campos [1*]**, Wayne Hocking**[2]**, and Frédéric Fabry**[1]
[1]*Department of Atmospheric and Oceanic Sciences, McGill University, Montreal, Quebec, Canada*
[2]*Department of Physics, University of Western Ontario, London, Ontario, Canada*

1. INTRODUCTION

In a typical setting for VHF-ST radars (Figure 1), a known pulse of power P_{Tx} is sent from the transmitter hardware towards the antennas. Actual antennas also have power losses, in particular due to thermal-energy dissipation in the antenna structure and cables. Therefore, the power radiated to space P_t is actually smaller than the power available at the antenna input P_{Tx}. The ratio of these quantities is the antenna radiation efficiency (or loss factor, $e_a = P_t /P_{Tx}$). Similar power losses are also experienced during the antenna reception, between the backscattered-power input at the antenna (P_r) and the power output from the antenna towards the receiver hardware (P_{Rx}). Consequently, $e_a = P_r /P_{Rx}$. On the other hand, the transmitter could leak small amounts of power into the receiver, cables, and antenna structure, generating electromagnetic noise at the radar VHF frequency. These leaked powers (expressed here as antenna noise N_a and Receiver Noise N_{Rx}) can be particularly significant during the radar reception period. We then have a useful expression:

$$P_r \ e_a + N_a = P_{Rx} \quad . \tag{1}$$

Of further relevance, however, is the fact that the power output after signal processing (P_{out}) is usually given in arbitrary units. Inside the receiver system, there is an analog-to-digital converter (ADC) that changes the measured power from Watts to the arbitrary units (au) of the ADC. The receiver system includes the power P_{Rx} output by the antennas into the receiver hardware, the analog-to-digital converter ADC, and the signal processing in the computer, finishing at P_{out} (i.e., the power output by the computer after signal processing). In the linear region of a receiver with linear amplifiers, the conversion from Watts to arbitrary units is mathematically expressed by the receiver efficiency, e_{Rx}, such that

$$P_{Rx} \ e_{Rx} + N_{Rx} = P_{out} \quad . \tag{2}$$

* *Corresponding author address:* Edwin F. Campos, McGill University, Dept. of Atmospheric & Oceanic Sciences, 805 Sherbrooke Street West, Montreal, Quebec, Canada.   H3A-2K6;   e-mail: ecampos@zephyr.meteo.mcgill.ca .

Measurement or retrieval of several meteorological variables (such as precipitation intensity) requires that P_{out} must be given in Watts instead of au. Radar calibration is a central issue that must be addressed before attempting any quantitative interpretation of precipitation radar measurements in the VHF band. Any radar power calibration involves a comparison between a known power source and the radar power measurement. In a standard calibration method, the known power source corresponds to the input (in Watts) from a noise-generator. For a less common calibration method, the known power source is the cosmic radio emissions (in Watts). We discuss both calibration methods applied to data taken by the McGill VHF radar.

2. METHODS
2.1. Noise-generator calibration

Let us have a power P_{NG} from a noise-generator hardware (*N-G*) that was input into the Receiver *Rx*. This power was digitized by the Analog-to-Digital Converter (*ADC*) and then sent to a computer, where the signal processing took place. This gave as a result the output power P_{out}. The objective here was to obtain a linear relation between the power input by the noise-generator (P_{NG}, in Watts) and the radar power output after all signal processing (P_{out}, in au); i.e.,

$$P_{out} \ B_{NG} + A_{NG} = P_{NG} \quad ; \tag{3}$$

where A_{NG} is the power (noise) generated within the hardware, measured in Watts. B_{NG} corresponds to the conversion factor between the input and output powers, measured in W/au. It should be noticed that this calibration did not take into account any antenna parameters (e.g., efficiency and noise).

2.2. Sky-noise calibration

If the power received by the radar antennas comes exclusively from cosmic sources, then a linear relation can be obtained between the VHF cosmic radio emissions (sky power: $P_{sky} = P_r$, in Watts) and the radar output power (P_{out}, in au); i.e.,

$$P_{out} \ B_{sky} + A_{sky} = P_{sky} \quad ; \tag{4}$$

where A_{sky} corresponds to the power (noise) generated within the radar hardware, measured in Watts. B_{sky} (measured in W/au) is the conversion factor between the power received by the antennas and the power output after the signal processing. The values of P_{sky}

were obtained from sky surveys of cosmic radio emissions at VHF. These sky surveys are usually given as brightness temperatures (T_1) valid for a given electromagnetic frequency (f_1). This survey frequency is hardly ever equal to the electromagnetic operation frequency of our radar (f_2). Therefore, we had to correct these brightness temperatures before applying them in our calibration. The sky brightness temperature corresponding to our radar (T_2) is then given by [e.g., *Roger et al.*, 1999, page 14; or *Campistron et al.*, 2001, equation 3]

$$T_2 = T_1 \left(\frac{f_2}{f_1} \right)^{-b} \quad ; \qquad (5)$$

where the brightness temperatures are both given in degrees Kelvin, and ß is the so-called spectral index. Although ß varies according to the position in the sky as well as the ratio f_2/f_1, it is generally assumed that ß= 2.5, which leads to a relative error smaller than 3% in the retrieved temperature [*Campistron et al.*, 2001].

Then, the cosmic power (in Watts) at 52 MHz is given by [e.g., *Ulaby et al.*, 1981, section 4.4]

$$P_{sky} = k_{Boltzmann} T_2 BPF_{width} \quad ; \qquad (6)$$

where $k_{Boltzmann}$ = 1.381x10^{-23} J/K is the Boltzmann constant [e.g., *Mohr and Taylor*, 2003], and J/K = W / (Hz K). BPF_{width} is the band-pass filter width of the radar receiver, in Hertz.

This sky-noise calibration only provided information about the antenna and receiver parameters in a general sense. Particular values such as antenna efficiency or receiver noise could not be retrieved in this manner. However, we were able to retrieve these antenna and receiver parameters by combining both the sky-noise calibration and noise-generator calibration methods. The next section explains the procedure.

2.3. Radar operation

To show the application of our method we used data from the McGill VHF radar working under the configuration described in Table 1. The signal processing used here was the same as in *Hocking* [1997, section 4]. Every 35 seconds, a profile of 45 Doppler power spectra (300-point discrete-spectrum within a spectral range of ± 10.0 Hz, for 45 range gates between 0.5 and 23.0 km) was produced. We integrated each of these spectra in order to obtain corresponding P'_{out} values; i.e., the integrated powers (in au) within the Doppler spectral range (*DSR*, see Table 1). Notice that we do not store the full Doppler power spectra, but only the section within the DSR. However, we know that the full spectral range is defined by the radar sampling rate:

$$f_{sampling} = \frac{PRF}{NCI} \quad ; \qquad (7)$$

where *PRF* is the radar pulse repetition frequency and *NCI* is the number of coherent integrations (given in Table 1). The full spectral range corresponds to Doppler frequencies within ± 0.5 $f_{sampling}$. Then, the quantity P_{out}, corresponding to the full spectral range, is given by

$$P_{out} = P'_{out} \frac{f_{sampling}}{DSR} = \frac{P'_{out} \times PRF}{DSR \times NCI} \quad . \qquad (8)$$

Table 1. McGill VHF Radar parameters

Parameter	Value
Beam direction	vertical
Tx wavelength (frequency)	5.77 m (52.0 MHz)
Peak Tx power	40 kW
One-way half-power half-beamwidth	2.3 degrees
Pulse duration	3.5 µs
Pulse repetition frequency (*PRF*)	6.0 kHz
Band pass Rx filter width (*BPF$_{width}$*)	400 kHz
Number of coherent integrations (*NCI*)	16
Doppler spectral range (*DSR*, after signal processing)	20.0 Hz
Pulse coding	None (i.e., monopulse)
Time resolution	35 s / profile

As described in section 2.1, during the noise-generator calibration, a small modification was made in the reception hardware. The noise-generator output was connected to the receiver, just after the transmitter-receiver switch (instead of this switch). Then, different noise sources were obtained by changing the factor *F* in the noise-generator hardware. One unit increment in *F* was equivalent to a 290 Kelvins increase in brightness temperature. At *F* = 0, the noise generator enter a small amount of power into the receiver. This amount depends on the noise generator temperature (approximately 290 K) in a manner similar to equation (6). Therefore, power input by the noise generator into the radar receiver was given by:

$$P_{NG} = (F+1)(290\,K)\,k_{Boltzmann}\,BPF_{width} \quad ; \qquad (9)$$

where P_{NG} is the noise-generator power (in Watts, measured in the radar receiver just after the band-pass filter). As before, $k_{Boltzmann}$ is the Boltzmann constant and BPF_{width} is the band-pass filter width of the radar receiver (given in Table 1), in Hertz.

For the second part of our calibration, there was no need to disconnect the transmitter, or to alter the normal operation of the radar in any way. We kept the radar hardware and software working as usual (Figure 1). The known power sources from cosmic radio emissions (in Watts) were then compared with the corresponding radar integrated power (in au) measured only at very high range gates (between 17.5 and 22.5 km). At these ranges, backscattering of the transmitted power and other terrestrial VHF radio sources is negligible. Thus, the radar received powers -at these high ranges only- were considered as coming from cosmic sources only. The details are given in the next section.

3. RESULTS
3.1. Noise-generator calibration

The noise-generator calibration was performed using observations made on 21 October 2004. The results are presented in Figure 1, where the left Y-axis gives the noise-generator factor F, and the right Y-axis gives the known input power P_{NG} [computed from equation (9)]. For a given P_{NG} value, there are 45 P_{out} values plotted in the X-axis. These P_{out} values correspond to the 45 radar range gates (between 0.5 and 23.0 km). The range of F values, from 0 to 30 units, was sampled two times (the two datasets are represented in Figure 1 by crosses and circles). A Chi-square linear fit [*Press et al.*, 1986, section 14.2] was then used to obtain the relation

$$P_{NG} = \left(-3.420x10^{-15} \pm 6.7\times10^{-17}\right)[W] + \\ P_{out}\left(9.250x10^{-21} \pm 2.3\times10^{-23}\right)[W/au] \quad ; \tag{10}$$

where the units are given in square brackets, and the uncertainties correspond to one standard-deviation errors in the coefficients estimates. The relationship (10) is presented as a line in Figure 1.

3.2. Cosmic-Noise calibration
3.2.1. Sky map

The cosmic noise power P_{sky} at the radar operating frequency (52 MHz) was obtained from a sky brightness temperatures map at 22 MHz. We used the map given by *Roger et al.* [1999]. The original map resolution is 1 minute (of an hour) in right ascension and 15 minutes (of a degree) in declination. However, considering our radar beam width and time resolution, the radar observations and the sky map did not match in resolution. Therefore, the sky brightness temperatures were smoothed in order to resemble our VHF radar resolution. We did this by convolving the *Roger et al.*'s sky map with a two-dimensional Gaussian function (as an approximation of the antenna polar diagram). This is a function of maximum amplitude equal to one and half-amplitude half-beam width equal to 2.3 degrees (i.e., our radar one-way half-power half-beamwidth, given in Table 1). This Gaussian function was spread over a 37x37 elements matrix, corresponding to angles between -4.625º and +4.625º (i.e., near two times the radar half-power beam width). In addition, the sky

brightness temperatures by *Roger et al.* are given in epoch-B1950 equatorial-coordinates. These coordinates, right ascension and declination are continuously changing in time, primarily as a result of the precession of the equinoxes. We then had to convert the figure coordinates from the epoch B1950 to the current epoch J2000. For this, we used the standard procedure given in section B42 of The Astronomical Almanac [*Nautical Almanac Offices*, 2003].
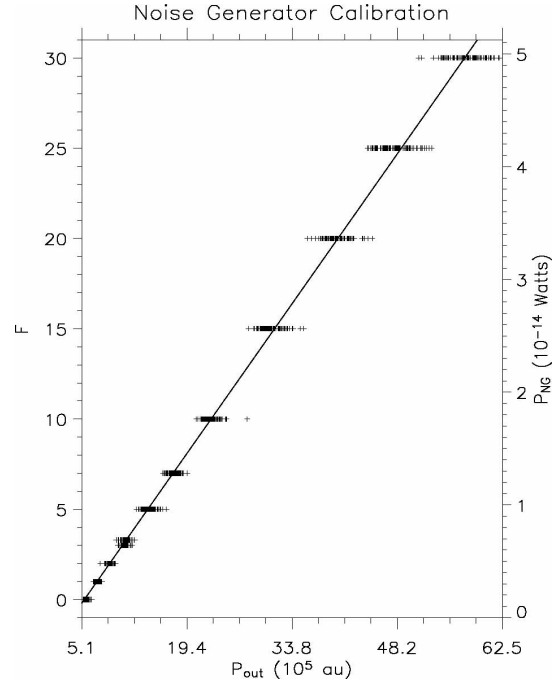
Figure 1. *Noise-generator calibration. The left-side Y-axis is the noise-generator factor F, which is related to the right-side Y-axis, the power P_{NG}, by equation (19). For a P_{NG} value, there are 45 P_{out} values (corresponding to 45 radar range gates) plotted in the X-axis. The linear relation in equation (20) is given by the line, and it is obtained from two calibration experiments (990 observations in total).*

3.2.2. Sky noise

Between 14 and 17 October 2004, the McGill VHF radar was operated according to the specifications given in Table 1. We selected the period in Figure 2, where the sky noise was coming only from cosmic sources. Notice that the temporal evolution of the sky noise power has a 23-hours-56-minutes cycle (i.e., a sideral day). This confirms the dominant cosmic origin of the noise observed by our VHF radar. From the measured Doppler power spectra, we computed the total integrated power (for spectral Doppler frequencies between -10.0 Hz and +10.0 Hz) at ranges between 17.5 and 22.5 km. At these high ranges, the Doppler power spectra received by VHF-ST radars are basically

formed by white noise, and when we integrate these spectra we obtain the so-called sky noise.
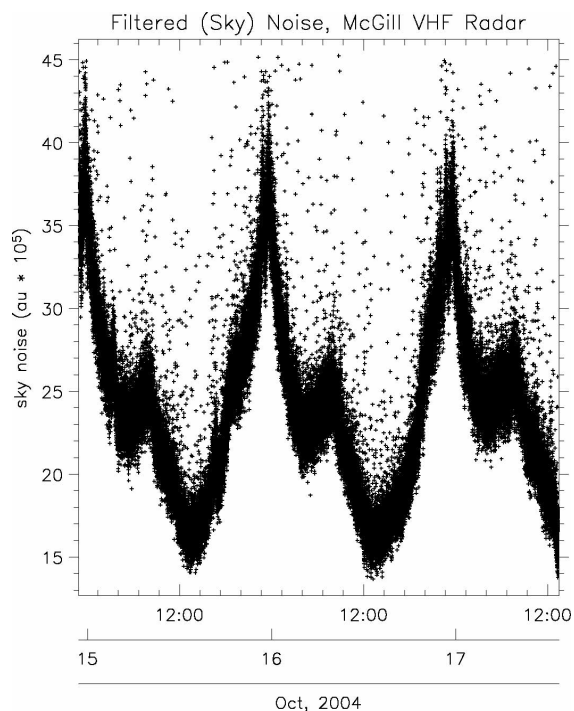
Figure 2. *Sky noise from cosmic sources. Example of power (sky-noise within the Doppler spectral range) measured by the McGill VHF-ST radar, with the beam at vertical direction, at ranges between 17.5 and 22.5 km, from 14 (starting at 22:50 UTC) to 17 (ending at 13:30 UTC) October, 2004. In total, 68,364 observations are plotted.*

By knowing the direction in the sky at which our radar is pointing at a given time, we can compute the equatorial coordinates of this direction. We computed the radar pointing directions (for the 12 cosmic sky-noise periods) using standard astronomical procedures valid for the epoch J2000 [e.g., *Lang*, 1999]. Since our radar was located at a fixed longitude and elevation angle (vertical direction), our cosmic sky noises correspond to a fixed declination with varying right ascension. This is shown in Figure 3, where the VHF cosmic sky-noises (black and blue crosses, in 10^5 au) are plotted as a function of right ascension. Since our radar measurements correspond to a declination of 45.41 degrees, we can compare our integrated powers with the corresponding sky brightness temperatures derived from the *Roger et al.'s* map (at the dashed line). This is also done in Figure 3, where the 52 MHz sky brightness temperatures [computed from equation (5) and the corresponding sky map values] are over-plotted as red crosses (in kiloKelvins). Notice that brightness temperatures are not considered at right ascensions between 19 and 21 hours. The reason is that the *Roger*

et al.'s sky map have removed the strong signal from Cygnus A, and the convolution of this sky map with the Gaussian function generates spurious data around Cygnus A.

Notice also that the radar sky-noise observations between 1 and 8 hours tend to be below the corresponding sky brightness temperatures. In principle, similar kind of underestimations are associated to ionospheric absorption of radio waves, which affects cosmic radiation when crossing the D and E ionospheric layers (at near 100 km altitude). Ionospheric absorption is a well-known phenomenon, which is controlled by solar activity (i.e., sun spot number). However, ionospheric absorption is not the explanation in this case, since the daytime period for this observations is between 11:10 and 22:03 UTC (i.e., between right ascension hours).
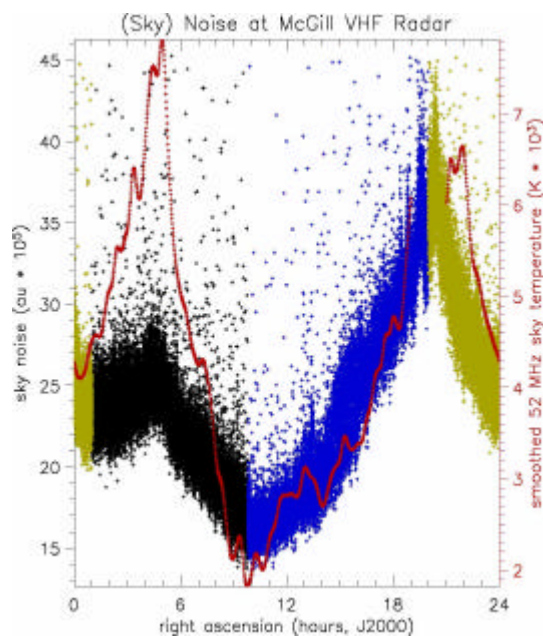
Figure 3. *Cosmic sky noise measured by the McGill VHF radar. The black, blue, and red crosses correspond to radar measurements in Figure 2 Black crosses were measured between 1 UTC and 9.8 right ascension hours, with 28,795 observations in total. The blue crosses correspond to 23,292 observations taken between 9.8 UTC and 20.0 right ascension hours. The green crosses (a total of 16,277 observations) were measured during the remaining right ascension periods. The red crosses are obtained from a sky brightness temperature map at a declination of 45.41°, (Roger et al., 1999, excluding the region around Cygnus A) and the equation (5).*

Furthermore, we identify three different regions in the sky-temperature map where the comparison with our radar measurements of sky noise is distinctive. (We will

explain the distinctive aspect of each region below.) The first region is located between 1.0 and 9.8 right ascension hours (black crosses in Figure 3), the next period corresponds to right ascension hours between 9.8 and 20.0 (blue crosses in Figure 3), and the remaining right ascensions is associated to the last region (green crosses in Figure 3).

In order to obtain the sky-noise powers, the brightness temperatures (red crosses) in Figure 3 were multiplied by the Boltzman constant and the radar Band-Pass-Filter width [i.e., equation (6)]. However, the radar measurements in Figure 3 still had a large amount of scatter, which could complicate the derivation of equation (4). We reduced this scatter in the following manner: for each P_{sky} observation (in Watts), we selected all radar observations (black, blue, and green crosses in Figure 3, in arbitrary units) that were within ± 30 seconds around the P_{sky} hour angle. (Recall that the resolution of the P_{sky} observations is 1 minute.) The median of these radar observations was then the radar output power, P_{out}, to be matched to the P_{sky} observation. The matched pairs are shown in Figure 9 by plotting P_{sky} as a function of P_{out}. This leads to the scatter plot in Figure 4 and the linear relation for Watts as a function of arbitrary units (the line in Figure 4).
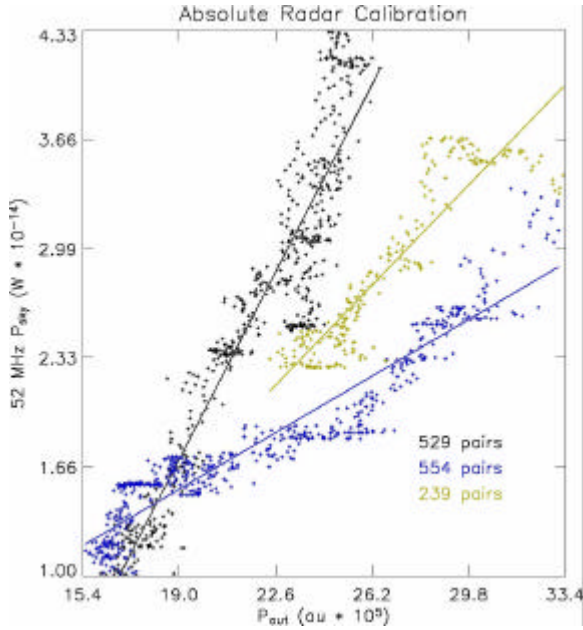
Figure 4. *Scatter plot of expected versus measured cosmic sky-noise power. The Y-axis values (P_{sky}, in 10^{-14} Watts) correspond to the red crosses in Figure 9. The X-axis values (P_{out}, in 10^5 au) are from the corresponding black, blue, and green crosses in Figure 3. The line corresponds to equations (11).*

As described in section 2.2, we expect a linear relation between P_{sky} and P_{out}. Accordingly, a linear relation between Watts and arbitrary units was derived, for each period in Figure 3, by minimizing the Chi-square error statistic, as in *Press et al.* [1986, section 14.2]. However, uncertainties in the sky map and in ß [i.e., equation (5)] depart the P_{sky} vs. P_{out} relationship from the linear function. In fact, we can recognize (although somehow arbitrarily) three distinctive linear relationships:

$$P_{sky} = \left(-4.318 \times 10^{-14} \pm 1.2 \times 10^{-15}\right)[W] + P_{out}\left(3.174 \times 10^{-20} \pm 5.3 \times 10^{-22}\right)[W/au] \tag{11a}$$

for 1.0 hours = right ascension < 9.8 hours;

$$P_{sky} = \left(-2.910 \times 10^{-15} \pm 3.1 \times 10^{-16}\right)[W] + P_{out}\left(9.572 \times 10^{-21} \pm 1.4 \times 10^{-22}\right)[W/au] \tag{11b}$$

for 9.8 hours = right ascension < 20.0 hours; and

$$P_{sky} = \left(-1.667 \times 10^{-14} \pm 1.4 \times 10^{-15}\right)[W] + P_{out}\left(1.695 \times 10^{-20} \pm 5.1 \times 10^{-22}\right)[W/au] \tag{11c}$$

for the remaining right ascension hours. As before, the relationship units for equations (11) are given in square brackets, and its uncertainties correspond to one standard-deviation errors in the coefficients estimates. These three distinctive relationships then lead us to identify three distinctive regions in the sky map.

4. DISCUSSION

Around 45.41º declination angles, the sky map by *Roger et al.* [1999] is not adequate to produce our radar calibration (it does not resemble the shape of the radar-measured sky-noise). However, we could identify certain useful regions in any given sky map by combining results from sky-noise and noise-generator calibrations. In fact, the ratio of the slopes derived from each method provide the value of the antenna efficiency, i.e.,

$$e_a = \frac{B_{NG}}{B_{sky}}. \tag{12}$$

Then, considering that a typical value for e_a for ST-VHF radars is around 0.7 (i.e. 70% efficiency) or less, we can estimate which region in a sky map produces antenna efficiencies in this order of magnitude.

From equations (10), (11), and (12), we found in our dataset that:

e_a = 0.29, for 1.0 hours = right ascension < 9.8 hours;
e_a = 0.97, for 9.8 hours = right ascension < 20.0 hours; and e_a = 0.54, for the remaining right ascension hours.

Therefore, the last efficiency is the only reasonable value (i.e., 54% is close to the expected value of about 70%, 97% is a too high value and 29% is too low). This suggest that the region with 20.0 hours = right

ascension < 1.0 hours (green crosses in Figure 3) is the most adequate for our calibration purposes . However, an independent measurement of the antenna efficiency is required in order to validate this result.

When dealing with the power measured by VHF-ST radars, it is often necessary to convert power units (from the arbitrary units of the analog-to-digital converter) into Watts. A so-called absolute calibration is then required. This paper discussed two methods of obtaining this calibration: the noise-generator calibration and the sky-noise calibration methods. There are important inconvenients associated with using exclusively one or the other. The noise-generator method requires hardware (the noise generator) that is not always available at the radar site, and the normal operation of the radar has to be interrupted to connect this hardware. Furthermore, the calibration equation that results does not take into account the antenna losses, and is therefore not accurate. On the other hand, attempts to calibrate VHF radars using the sky-noise method have only been reported a few times in the literature [e.g., *Hocking et al.*, 1983; *Green et al.*, 1983; *Campistron et al.*, 2001). It is difficult to obtain accurate reference sources of cosmic radiation at VHF band. As well, in terms of its methods, a calibration from known sources of cosmic radiation is more elaborated than a calibration from a noise generator. Furthermore, sky-noise calibration-methods do not provide independent information on the receiver or antenna parameters. This information on radar parameters is fundamental when applying the radar equation to derive meteorological variables such as precipitation.

In order to overcome these calibration difficulties , we suggest a new approach towards the ST radar calibration, which implies a combination between the sky-map and noise-generator methods. This new approach is currently under development by our group.

References

Campistron, B., G. Despaux, M. Lothon, V. Klaus, Y. Pointin, and M. Mauprivez, 2001: A partial 45 MHz sky temperature map obtained from the observations of five ST radars. *Annales Geophysicae*, *19*(8), 863-871.

Green, J. L., W. L. Clark, J. M. Warnock, and K. J. Ruth, 1983: Absolute calibrations of MST/ST Radars, in *Preprints of the 21st Conference on Radar Meteorology, Edmonton, Alta., Canada*, pp. 144-147, American Meteorological Society, Boston, Massachusetts, USA.

Hocking, W. K., 1997: System design, signal -processing procedures, and preliminary results fro the Canadian (London, Ontario) VHF atmospheric radar, *Radio Science*, *32*(2), 687-706.

Hocking, W. K., G. Schmidt, and P. Czechowsky, 1983: Absolute Calibration of the SOUSY VHF Stationary Radar, *Internal Report MPAE-W-00-83-14*, 16 pp., Max-Planck-Institut für Aeronomie, Katlenburg-Lindau, Germany.

Lang, K. R., 1999: *Astrophysical Formulae, Vol. II: Space, Time, Matter and Cosmology*, 3rd Enlarged and Revised Edition, 436 pp., Springer-Verlag, Berlin, Germany.

Mohr, P. J., and B. N. Taylor: 2003: The Fundamental Physical Constants, *Physics Today*, *56*(8), BG6-BG13, American Institute of Physics, Melville, NY, USA.

Nautical Almanac Offices, US Naval Observatory, and UK Rutherford Appleton Laboratory, 2003: *The Astronomical Almanac for the year 2003*, U.S. Naval Observatory, Washington, D.C., USA.

Press, W. H., B. P. Flannery, S. A. Teukolsky, and W. T. Vetterling, 1986: *Numerical Recipes: The Art of Scientific Computing*, 818 pp., Cambridge University Press, New York, USA.

Roger, R. S., C. H. Costain, T. L. Landecker, and C. M. Swerdlyk, 1999: The radio emission from the galaxy at 22 MHz, *Astronomy and Astrophysics Supplement Series*, *137*(1), 7-19.

Ulaby, F. T., R. K. Moore, and A. K. Fung, 1981: *Microwave remote sensing active and passive, Volume 1: Microwave Remote Sensing Fundamentals and Radiometry*, 456 pp., Addison-Wesley Publishing Company, Massachusetts, USA.